

Electrical properties of ferroelectric BaTiO₃ thin film on SrTiO₃ buffered GaAs by laser molecular beam epitaxy

Cite as: Appl. Phys. Lett. **94**, 032905 (2009); <https://doi.org/10.1063/1.3075955>

Submitted: 29 September 2008 . Accepted: 07 January 2009 . Published Online: 23 January 2009

W. Huang, Z. P. Wu, and J. H. Hao



View Online



Export Citation

ARTICLES YOU MAY BE INTERESTED IN

Properties of epitaxial BaTiO₃ deposited on GaAs

Applied Physics Letters **102**, 012907 (2013); <https://doi.org/10.1063/1.4773988>

Hetero-epitaxy of perovskite oxides on GaAs(001) by molecular beam epitaxy

Applied Physics Letters **85**, 1217 (2004); <https://doi.org/10.1063/1.1783016>

In-plane dielectric properties of epitaxial Ba_{0.7}Sr_{0.3}TiO₃ thin films grown on GaAs for tunable device application

Journal of Applied Physics **112**, 054110 (2012); <https://doi.org/10.1063/1.4749270>

Lock-in Amplifiers

Find out more today



Zurich Instruments

Electrical properties of ferroelectric BaTiO₃ thin film on SrTiO₃ buffered GaAs by laser molecular beam epitaxy

W. Huang, Z. P. Wu, and J. H. Hao^{a)}

Department of Applied Physics and Materials Research Centre, The Hong Kong Polytechnic University, Hong Kong, People's Republic of China

(Received 29 September 2008; accepted 7 January 2009; published online 23 January 2009)

Ferroelectric BaTiO₃ thin films were epitaxially grown on (001) GaAs substrate using SrTiO₃ as a buffer layer by laser molecular beam epitaxy. The perovskite SrTiO₃ buffer layer present a body centered cubic structure by formation of an interfacial layer with the [100]SrTiO₃||[110]GaAs in-plane relationship. Thereupon, a highly *c*-oriented BaTiO₃ thin film was grown on SrTiO₃/GaAs in a layer by layer mode. Enhanced electrical properties of the heteroepitaxial structure were demonstrated. The BaTiO₃(150 nm)/SrTiO₃/GaAs system demonstrates hysteresis loops with a remnant polarization of 2.5 μC/cm² at 600 kV/cm and a small leakage current density of 2.9 × 10⁻⁷ A/cm² at 200 kV/cm. © 2009 American Institute of Physics. [DOI: 10.1063/1.3075955]

III-V semiconductors such as GaAs have direct band gap and higher saturated electron mobility compared to Si. Great efforts have been made to develop GaAs-based metal-ferroelectric-insulator-semiconductor (MFIS) functional heterostructure.¹⁻³ Much research has been focused on the electrical properties of amorphous and polycrystalline MFIS structure via a buffered insulator layer.⁴⁻⁶ The epitaxial growth of perovskite titanate thin films on Si has been studied extensively in the last decades.⁷⁻⁹ Integration with GaAs has attracted much less attention. Murphy *et al.*⁵ reported the ferroelectric properties in epitaxial grown BaTiO₃ (BTO) on GaAs via MgO buffer and found that these properties are greatly sensitive to the interface structure and buffer thickness. Chen *et al.*⁶ reported that optical waveguiding was observed in BTO/MgO/Al_xO_y/GaAs structure showing primary optical confinement in the BTO thin film. Recent study showed that the MgO with a thickness of a few nanometers on GaAs may suffer from the high charge injection while increasing reverse bias voltage due to a MgO/GaAs interface current effect.¹⁰ Ferroelectric oxides on MgO buffered GaAs exhibits weak ferroelectric properties with a large leakage.⁵ Compared with MgO, SrTiO₃ (STO) with a cubic perovskite structure has a relatively large dielectric constant and low loss.¹¹ STO has also widely been used as a suitable interface template for the growth of high-quality functional oxides.¹²⁻¹⁴ So far, the epitaxial thin film of STO grown on GaAs has only been achieved via a complex molecular beam epitaxy (MBE) with a submonolayer of titanium as buffer.¹⁵ In this work, we employ O₂ flowing laser MBE technique to grow epitaxial BTO thin films on STO/GaAs.

The BTO/STO/GaAs (001) heterostructure was grown by O₂ flowing pulsed laser MBE system with an operation wavelength of KrF (λ=248 nm). The laser energy density was about 6 J/cm² at a frequency of 1 Hz. A system of reflective high energy electron diffraction (RHEED) was used to monitor the film growth process. As our recent report,¹⁶ STO layer was first deposited on GaAs (001) substrates at 600 °C. During the deposition, the chamber was evacuated to a base pressure of 5 × 10⁻⁵ Pa to avoid

oxidation of the GaAs substrate, although the GaAs surface reacts less severely with oxygen in comparison with Si. Then, the buffered GaAs was heated to 650 °C and the subsequent ferroelectric BTO film was grown under a flowing O₂ atmosphere of 1 Pa. The deposited films were then *in situ* annealed in ambient of high oxygen pressure before being cooled down to room temperature. Finally, Pt electrodes were deposited for electrical measurements. *P*-type GaAs was used as a bottom electrode in our measurement. The resistivity of used GaAs wafer was estimated to be 2–6 Ω cm. The film structure was determined by x-ray diffraction (XRD) and the interface characteristic was investigated by transmission electron microscopy (TEM). The dependence of current density on electrical field (*J*-*E*) of the system was measured. The ferroelectric properties were measured by using a ferroelectric test system (Radiant Inc.).

The RHEED patterns (Fig. 1) show the epitaxial features of BTO films grown on GaAs substrates using STO as a buffer layer. The diffraction spots of GaAs representing (002) plane cluster in Fig. 1(a) gradually faded away as the STO started to grow. Figure 1(b) shows the diffraction pattern with two unit cell of STO (about 8 Å), indicating the film was coherent at the onset of the STO growth. Then two elongated bright spots emerging with a wider separation

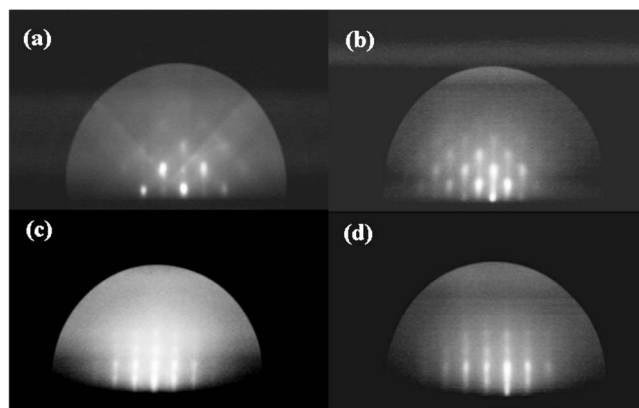


FIG. 1. RHEED patterns for heteroepitaxial growth of BTO thin films on GaAs via STO buffer layer at various thicknesses: (a) 0 Å STO, (b) 8 Å STO, (c) 30 Å STO, and (d) 200 Å BTO.

^{a)} Author to whom correspondence should be addressed. Electronic mail: apjhao@polyu.edu.hk.

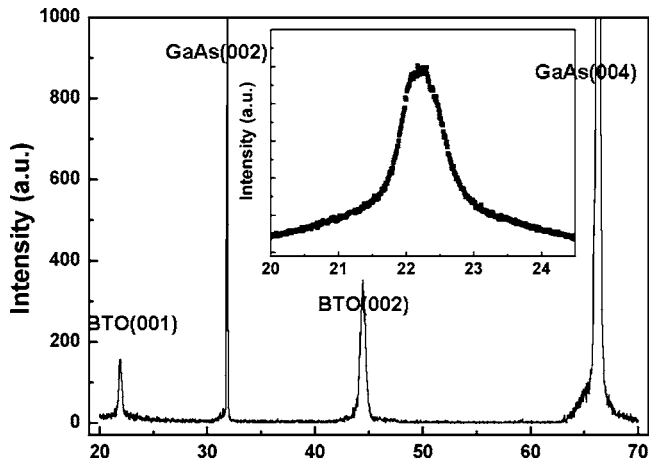


FIG. 2. XRD pattern of the heteroepitaxial growth BTO films on STO buffered GaAs (001). The inset shows the rocking curve of BTO (002).

could be observed. According to Bragg's diffraction law, STO unit began to grow with a 45° in-plane rotation on GaAs to get a comfortable lattice match due to a large mismatch between STO ($a=3.905 \text{ \AA}$) and GaAs ($a=5.65 \text{ \AA}$), which is consistent with the observation in Ref. 15. The spotty diffraction pattern in Fig. 1(b) also suggests that STO possibly grew in coherent two-dimensional-island behavior at the STO/GaAs interface, which may be due to the large number of dislocations due to mismatch strain between STO and GaAs. This coherent behavior remained with film thickness of up to approximately 30 \AA as shown in Fig. 1(c), then the spot gradually faded away when the thickness was greater than 30 \AA , suggesting that the STO film began to relax when the growth went beyond this thickness. For the subsequent growth of BTO film on STO buffered GaAs, conspicuous streaky diffraction patterns of the (001) plane of BTO could be observed in Fig. 1(d). This unchanged streaky diffraction pattern indicates that the growth of BTO becomes a two dimensional layer-by-layer growth on STO buffered GaAs. It also suggests that the smoothness and crystallinity of BTO film remained satisfactory via a STO interfacial layer. During the whole growth process, no unidentifiable RHEED patterns were detected.

Figure 2 shows a typical θ - 2θ XRD scan of the BTO/STO/GaAs heterostructure. Only the (00 l) peaks of the BTO appear in the diffraction patterns indicating that the BTO is basically c -axis oriented growth on STO buffered GaAs substrate. There is no apparent peak corresponding to STO in Fig. 2 due to the small thickness of STO layer. To further investigate the degree of in-plane orientations, Φ scan was performed (not shown here), which reveals that the BTO film is epitaxially grown on the (001) surface of STO and has an in-plane film-substrate orientation relationship of $[100]_{\text{BTO}} \parallel [100]_{\text{STO}} \parallel [110]_{\text{GaAs}}$. The BTO film on STO buffered GaAs has good single crystallinity, which is evident from the small full width at half maximum value of the rocking curve of (002) BTO (seen in inset of Fig. 2). In addition, the lattice constant c of BTO was then calculated to be 4.125 \AA , which is slightly larger than that of bulk BTO ($c=4.01 \text{ \AA}$) from powder diffraction. It suggests that the BTO film is slightly compressively strained by the underlying STO buffered layer ($a=3.903 \text{ \AA}$) and the interface of STO buffer layer considerably affects the BTO crystallographic structure. The cross-sectional TEM images in Fig. 3

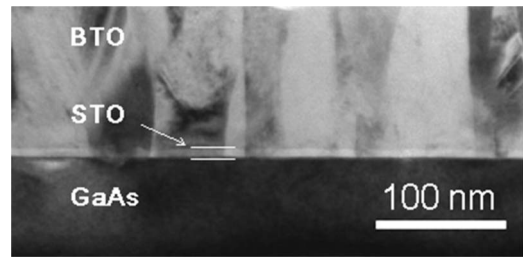


FIG. 3. Cross-sectional TEM image of the BTO/STO/GaAs heterostructure.

reveal a sharp interface structure of the heterostructure. It can be seen that the BTO film with uniform thickness of 150 nm has grown columnarly on a 10-nm -thick STO buffer layer.

In order to evaluate electrical properties of the BTO/STO/GaAs heterostructure for applications, the leakage current and polarization properties were measured as a function of electrical field. As shown in Fig. 4(a), the leakage current density J of the BTO/STO/GaAs heterostructure is considerably reduced by inserting STO buffer layer under a given electric field. For instance, the value of current density is $2.9 \times 10^{-7} \text{ A/cm}^2$ for BTO thin films deposited on a 10 nm STO buffer layer at a field of 200 kV/cm , almost two orders of magnitude lower than that ($1.7 \times 10^{-5} \text{ A/cm}^2$) for BTO thin films without using a STO buffer layer under the same field. However, obvious asymmetry was observed in the plot of the leakage current versus electric field. This feature may be attributed to interface states caused by stress-induced dis-

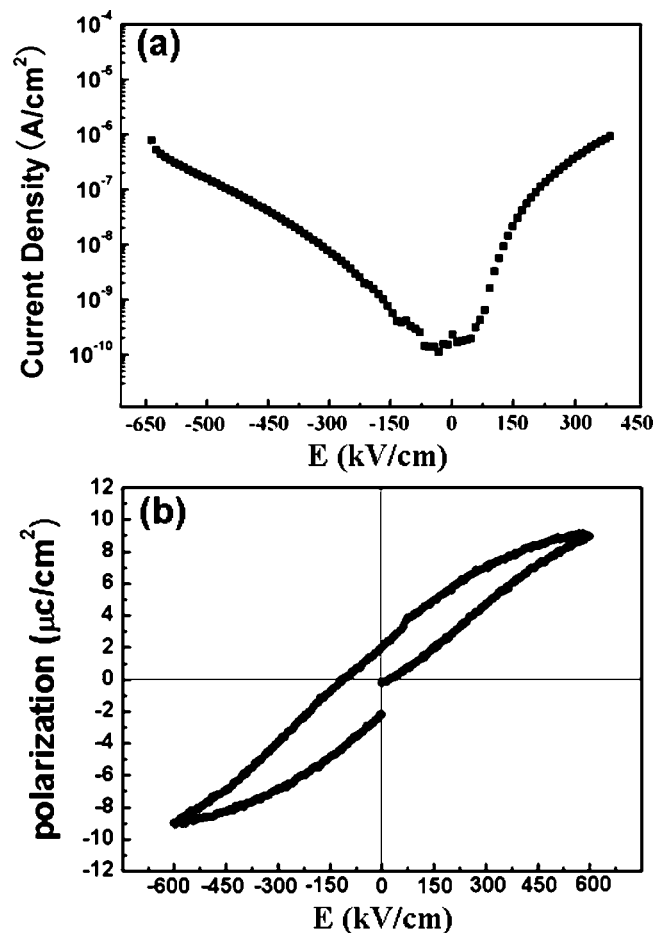


FIG. 4. Electrical and ferroelectric properties of the BTO/STO/GaAs heterostructure. (a) J - E property. (b) P - E loop.

location, which has also been reported in some metal-oxide-semiconductor structures.¹⁷ It is known that the microstructure in the vicinity of the film/substrate interface plays an important role in defining the leakage current in films. As an excellent isolating material, the STO buffer layer can effectively suppress the interdiffusion between BTO and GaAs. The P - E characteristics for varying applied electrical field are shown in the Fig. 4(b). Compared with previous reports on MgO buffered BTO film on GaAs,⁵ the BTO/STO/GaAs heterostructure exhibits a more saturating P - E loop with a remnant polarization (P_r) of about $2.5 \mu\text{C}/\text{cm}^2$ at the applied electric field of 600 kV/cm. Although the measured P - E loop windows are still smaller than the theoretical calculated values, the charge injection was significantly suppressed and the dielectric behavior is therefore enhanced. This is somewhat similar to the improved property in MFIS structures, such as BFO/ZrO/Si, SrBi₂Ta₂O₉/HfTaO/Si.^{18,19} The high structure-dependent films always show good performances by inducing a good interfacial layer. Therefore, the P - E loop with a small leakage current can also be considered and that the interface between BTO and GaAs is improved by inserting STO as buffer layer, and thus a good epitaxy of BTO layer exhibits enhanced electrical properties.

In conclusion, a technique of O₂ flowing laser MBE was used to grow heteroepitaxial structure of BTO/STO/GaAs. We found that structural and electrical properties of the heterostructure are greatly improved. The BTO/STO/GaAs prepared by laser MBE can serve as a model system of dielectric materials integrated with III-V semiconductors for a variety of applications.

This research was supported by a grant from the Research Grants Council of Hong Kong (GRF Project No. PolyU7025/05P).

- ¹M. Hong, J. Kwo, A. R. Kortan, J. P. Mannaerts, and A. M. Sergent, *Science* **283**, 1897 (1999).
- ²M. Passlack, J. Abrokwhah, R. Droopad, Z. Yu, C. Overgaard, S. Yi, M. Hale, J. Sexton, and A. Kummel, *IEEE Electron Device Lett.* **23**, 508 (2002).
- ³K. D. Choquette, K. M. Geib, C. I. H. Ashby, R. D. Twisten, O. Blum, H. Q. Hou, D. M. Follstaedt, B. E. Hammons, D. Mathes, and R. Hull, *IEEE J. Sel. Top. Quantum Electron.* **3**, 916 (1997).
- ⁴M. Hong, Z. H. Lu, J. Kwo, A. R. Kortan, J. P. Mannaerts, and J. J. Krajewski, *Appl. Phys. Lett.* **76**, 312 (2000).
- ⁵T. E. Murphy, D. Chen, and J. D. Phillips, *Appl. Phys. Lett.* **85**, 3208 (2004).
- ⁶D. Chen, T. E. Murphy, S. Chakrabarti, and J. D. Phillips, *Appl. Phys. Lett.* **85**, 5206 (2004).
- ⁷R. A. Mckee, F. J. Walker, and M. F. Chisholm, *Phys. Rev. Lett.* **81**, 3014 (1998).
- ⁸H. Li, X. Hu, Y. Wei, Z. Yu, X. Zhang, R. Droopad, A. A. Demkov, J. Edwards, Jr., K. Moore, W. Ooms, J. Kulik, and P. Fejes, *J. Appl. Phys.* **93**, 4521 (2003).
- ⁹J. H. Hao, J. Gao, Z. Wang, and D. P. Yu, *Appl. Phys. Lett.* **87**, 131908 (2005); J. L. Li, J. H. Hao, and Y. R. Li, *ibid.* **91**, 131902 (2007).
- ¹⁰J. C. Le Breton, S. Le Gall, G. Jézéquel, B. Lépine, P. Schieffer, and P. Turban, *Appl. Phys. Lett.* **91**, 172112 (2007).
- ¹¹C. Ang, L. E. Cross, Z. Yu, R. Guo, A. S. Bhalla, and J. H. Hao, *Appl. Phys. Lett.* **78**, 2754 (2001).
- ¹²S. Y. Yang, Q. Zhan, P. L. Yang, M. P. Cruz, Y. H. Chu, R. Ramesh, Y. R. Wu, J. Singh, W. Tian, and D. G. Schlom, *Appl. Phys. Lett.* **91**, 022909 (2007).
- ¹³J. Wang, H. Zheng, Z. Ma, S. Prasertchoung, M. Wuttig, R. Droopad, J. Yu, K. Eisenbeiser, and R. Ramesh, *Appl. Phys. Lett.* **85**, 2574 (2004).
- ¹⁴Y. Mukunoki, N. Nakagawa, T. Susaki, and H. Y. Hwang, *Appl. Phys. Lett.* **86**, 171908 (2005).
- ¹⁵Y. Liang, J. Kulik, T. C. Eschrich, R. Droopad, Z. Yu, and P. Maniar, *Appl. Phys. Lett.* **85**, 1217 (2004).
- ¹⁶Z. P. Wu, W. Huang, K. H. Wong, and J. H. Hao, *J. Appl. Phys.* **104**, 054103 (2008).
- ¹⁷F. Crupi, C. Ciofi, A. Germano, G. Iannaccone, J. H. Stathis, and S. Lombardo, *Appl. Phys. Lett.* **80**, 4597 (2002).
- ¹⁸Y. W. Chiang and J. M. Wu, *Appl. Phys. Lett.* **91**, 142103 (2007).
- ¹⁹X. B. Lu, K. Maruyama, and H. Ishiwara, *J. Appl. Phys.* **103**, 044105 (2008).